Experimental and theoretical investigations on the inhibition of mild steel corrosion in the ground water medium using newly synthesised bipodal and tripodal imidazole derivatives

ARTICLE *in* MATERIALS CHEMISTRY AND PHYSICS · OCTOBER 2014

Impact Factor: 2.26 · DOI: 10.1016/j.matchemphys.2014.05.033

6 AUTHORS, INCLUDING:

El-Sayed M. Sherif
King Saud University
113 PUBLICATIONS **1,929** CITATIONS
SEE PROFILE

Poomani Kumaradhas
Periyar University
82 PUBLICATIONS **288** CITATIONS
SEE PROFILE

Kavitha Louis
Central University of Tamil Nadu
105 PUBLICATIONS **986** CITATIONS
SEE PROFILE

Materials Chemistry and Physics 147 (2014) 572–582

Contents lists available at ScienceDirect

Materials Chemistry and Physics

journal homepage: www.elsevier.com/locate/matchemphys

Experimental and theoretical investigations on the inhibition of mild steel corrosion in the ground water medium using newly synthesised bipodal and tripodal imidazole derivatives

D. Gopi [a, b, *], El-Sayed M. Sherif [c, d], M. Surendiran [a], M. Jothi [e], P. Kumaradhas [e], L. Kavitha [f]

[a] Department of Chemistry, Periyar University, Salem 636 011, Tamilnadu, India
[b] Centre for Nanoscience and Nanotechnology, Periyar University, Salem 636 011, Tamilnadu, India
[c] Center of Excellence for Research in Engineering Materials (CEREM), Advanced Manufacturing Institute, King Saud University, P.O. Box 800, Al-Riyadh 11421, Saudi Arabia
[d] Electrochemistry and Corrosion Laboratory, Department of Physical Chemistry, National Research Centre (NRC), Dokki, 12622 Cairo, Egypt
[e] Department of Physics, Periyar University, Salem 636 011, Tamilnadu, India
[f] Department of Physics, School of Basic and Applied Sciences, Central University of Tamilnadu, Thiruvarur 610 101, Tamilnadu, India

HIGHLIGHTS

- Synthesis of new imidazole derivatives-BIDM(bipodal) and TITM(tripodal) inhibitors.
- Gravimetric analysis to investigate mild steel corrosion inhibition in ground water.
- Electrochemical characterizations to substantiate results of weight loss method.
- Quantum studies to analyse the chemical behavior, structure and substituent effect.

GRAPHICAL ABSTRACT

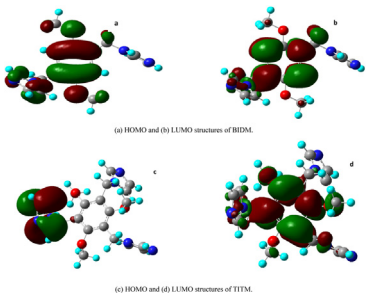

ARTICLE INFO

Article history:
Received 29 June 2013
Received in revised form
13 May 2014
Accepted 17 May 2014
Available online 11 June 2014

Keywords:
Metals
Computational techniques
Electrochemical techniques
Corrosion

ABSTRACT

Two new imidazole derivatives, namely 1,4-bis(*N*-imidazolylmethyl)-2-5-dimethoxybenzene (BIDM) and 1,3,5-tris(*N*-imidazolylmethyl)-2,4,6-trimethoxybenzene (TITM), were synthesised and their effects on the inhibition of mild steel corrosion in ground water medium are reported. The study was carried out using gravimetric and electrochemical techniques in order to determine the corrosion inhibition efficiencies of the bipodal and tripodal structured imidazoles. Further, the quantum chemical calculations using density functional theory (DFT) gave a profound insight into the inhibitory action mechanism of BIDM and TITM and their calculation parameters, such as E_{HOMO}, E_{LUMO} and ΔE were in good agreement with the results of the experimental studies. BIDM and TITM exhibited lowest corrosion current densities of circa 7.5 μA cm^{-2} and 4.1 μAcm^{-2} at the optimum concentrations of 0.67 and 0.49 mM, respectively. All measurements thus confirmed that both BIDM and TITM behaved as good inhibitors for mild steel corrosion in ground water medium.

* Corresponding author. Department of Chemistry, Periyar University, Salem 636 011, Tamilnadu, India. Tel.: +91 427 2345766; fax: +91 427 2345124.
E-mail address: dhanaraj_gopi@yahoo.com (D. Gopi).

http://dx.doi.org/10.1016/j.matchemphys.2014.05.033
0254-0584/

1. Introduction

Mild steel possesses good mechanical properties and it is a better economic alternative to its low cost [1]. Hence, it finds a wide industrial application as constructional materials in acid cleaning baths, water cooling systems, different refinery units pipelines, chemical operations, steam generators, ballast tanks, oil and gas production units [2–4]. On the other hand, the mild steel is easily prone to corrosion thereby, raised an intense desire to seek for an efficient corrosion inhibitor for this metal without any toxication of waterways in all water systems and industrial concerns.

Among the different corrosion prevention and protection methods [5–7], the use of chemical inhibitors is one of the best known methods of corrosion protection. Although there are continuing advances in the formulation of corrosion resistant materials, the uses of chemical inhibitors often remain the most practical and cost effective measures of preventing corrosion [1]. In precise, the efficiency of the inhibitors mainly depends on the nature of the metal surface, the structure of the inhibitor, which includes the number of adsorption active centres in the inhibitor molecule, their molecular size and the mode of adsorption [8–11].

Corrosion inhibitors are commonly, organic compounds with hetero atoms such as N, S, P, O, unsaturated bonds and aromatic planar cycles, which may aid to accept or donate electrons in order to get adsorbed on metallic surfaces by electrostatic interactions, interaction between the unshared pair of electrons of corrosion inhibitor and metal and interaction of electrons with metallic surface [12–21]. Among the several classes of heterocyclic compounds, imidazole derivatives were found as better inhibitors against corrosion for many metals and alloys in the ground water as well as other media.

In precise, the inhibition is assumed to occur via adsorption of the compound on the steel surface through active centres present in the molecule [17,22–24]. Thus the relationship between the adsorption of organic inhibitors, their molecular structure and enhancement in corrosion resistance related to the presence of the substituted groups has attracted the curiosity of many researchers [25–29]. The quantum chemical approach used in calculating the electronic properties of the imidazole molecule also ascertained the relation between inhibiting effect and molecular structure as the increased electron density around the inhibitor molecules through substitution have paved the way for improved inhibition efficiency.

Different electrochemical techniques such as open circuit potential (OCP), potentiodynamic polarization and electrochemical impedance spectroscopy (EIS) were usually employed to evaluate the inhibition mechanism for many decades. Whereas nowadays, a perfect exploration is attained with theoretical studies such as quantum chemical methods and molecular modelling techniques whose theoretical parameters obtained from the advanced hardware and software account for the molecular structure, reactivity, shape, binding properties and also mechanism of action in terms of chemical reactivity.

Thus the objective of the present work is to investigate the inhibition performance of the newly synthesised bipodal and tripodal imidazoles in preventing mild steel corrosion in the ground water environment. Ascertaining the corrosion inhibition on mild steel was done at different concentrations of BIDM and TITM by gravimetric analysis along with that of adsorption phenomenon and the results were correlated with that of the electrochemical techniques. Quantum chemical calculations were successively carried out to obtain the invaluable quantum chemical parameters such as E_{HOMO} and E_{LUMO} to understand the adsorption properties with respect to the structure of every individual molecule to attain a clear view on the relationship between the substituent effect and inhibition efficiency as well as molecular reactivity.

2. Materials and methods

2.1. Materials

Tests were performed on the mild steel samples (99.99% purity) of the following chemical composition (wt.%): C-0.13, P-0.032, S-0.025, Si-0.014, Mn-0.48 and Fe-balance. Specimens used in the weight loss experiment were mechanically cut into 4.0 cm × 2.0 cm × 0.2 cm dimensions. For electrochemical studies, specimens of size 1.0 cm × 1.0 × cm × 0.3 cm were cut, embedded in epoxy resin and mechanically ground with silicon carbide papers (from grades 120–1200) then followed by washing with double distilled water, degreasing with acetone, dried at room temperature and stored in moisture free desiccator before their use in corrosion studies.

2.2. Synthesis of imidazole derivatives

The NaOH solution of 25% (6.2 M) was added to a solution of imidazole (0.08 M) in CH_3CN and stirred for 10 min. To this solution, 1,4-bis(bromomethyl)-2,5-dimethoxybenzene (0.74 M) in acetonitrile was added at once and stirred at room temperature of 28 ± 1 °C for 48 h [30]. The reaction mixture was evaporated under reduced pressure and the residue obtained was extracted with CH_2Cl_2 (3 × 50 ml), washed with double distilled water (2 × 50 ml), brine (50 ml) and dried. The solvent was removed under vacuum and the residue was chromatographed using hexane/$CHCl_3$ (1:3) as eluent to give 1,4-bis(*N*-imidazolylmethyl)-2,5-dimethoxybenzene as a white solid.

In a similar synthetic way of BIDM, 1,3,5-tris(N-imidazolylmethyl)-2,4,6-trimethoxybenzene was synthesised as a white solid from imidazole (0.4 M) and 1,3,5-tris(bromomethyl)-2,4,6-trimethoxybenzene (17.14 M) using NaOH (6.4 M). The molecular structures of the as-synthesised imidazole derivatives are given in Fig. 1.

2.3. Characterization

The as-synthesized imidazole derivatives were purified and then characterized by ^1H and ^{13}C NMR spectra in $CDCl_3$ using deuterated dimethyl sulphoxide (DMSO) as internal standard on a JEOL GSX make with the frequency of 400 MHz NMR spectrometer. All the

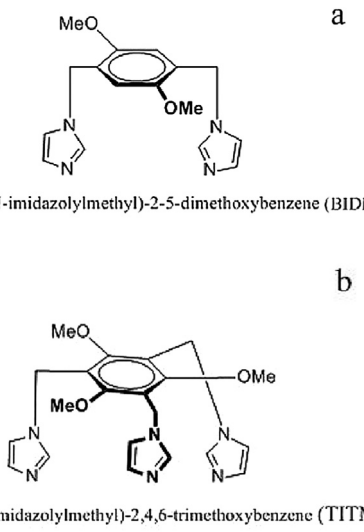

Fig. 1. Molecular structure of inhibitors (a) BIDM and (b) TITM.

reactions were carried out under nitrogen atmosphere. For 1,4-bis(N-imidazolylmethyl)-2-5-dimethoxybenzene (BIDM): ^{1}H NMR (400 MHz, $CDCl_3$): δ 3.73 (s, 6H), 5.08 (s, 4H), 6.49 (s, 2H), 6.93 (s, 2H), 7.06 (s, 2H), 7.55 (s, 2H) ppm; ^{13}C NMR (100 MHz, $CDCl_3$): δ 45.8, 56.0, 111.6, 119.4, 125.5, 129.4, 137.6, 150.9 ppm; EI-MS: m/z 298 (M^+); Anal. Calcd for $C_{16}H_{18}N_4O_2$: C, 64.41, H, 6.08, N, 18.78; Found: C, 64.66, H, 6.13, N, 18.70. For 1,3,5-tris(*N*-imidazolylmethyl)-2,4,6-trimethoxybenzene (TITM): ^{1}H NMR (400 MHz, $CDCl_3$): δ 3.53 (s, 9H), 5.05 (s, 6H), 6.86 (s, 3H), 6.96 (s, 3H), 7.50 (s, 3H) ppm; ^{13}C NMR (100 MHz, $CDCl_3$): δ 40.1, 63.0, 77.2, 119.0, 121.1, 129.4, 137.1, 160.1 ppm; EI-MS: m/z 408 (M^+); Anal. Calcd for $C_{21}H_{24}N_6O_3$: C, 61.75, H, 5.92, N, 20.58; Found: C, 61.78, H, 5.98, N, 20.75.

2.4. Electrolyte

Ground water was used as the electrolyte. A typical analysis of this electrolyte is given in our previous work [31]. Each experiment was carried out using the solutions obtained by dissolving the BIDM and TITM individually, with acetone. The concentrations of BIDM and TITM were varied from 0.17 to 1.01 mM and 0.12–0.74 mM, respectively in ground water medium.

2.5. Gravimetric analysis

In each experiment, the mild steel specimens were rinsed in deionised water and acetone, finally dried, then kept in a desiccator before their use in corrosion studies. The cleaned mild steel specimens were weighed and suspended in ground water at room temperature (28 ± 1 °C) for each inhibitor concentration for the period of 7 days (168 h). To determine the weight loss, the specimens were retrieved from test solutions after 7 days (168 h) [32,33]. Then as per the ASTM G1-03 designation "Standard Practice for Preparing, Cleaning, and Evaluating Corrosion Test Specimens" [34], the pickling operation was carried out at 80–90 °C by immersing in a 20% NaOH solution containing 200 g L^{-1} of zinc dust followed by scrubbing using bristle brush under running water so that the corrosion products could be removed, then dried and reweighed.

The weight loss can be calculated as the difference between the weight at the end of the given immersion test time (168 h) and the initial weight of the test coupon which was determined using the Shimadzu AUX 320 digital balance of ±0.1 mg sensitivity. The experiments were repeated thrice and the mean values of the weight loss were recorded. The corrosion rate obtained from weight loss, ν_w of the mild steel in the ground water containing different concentrations of inhibitors was studied as per the following Equation (1) [35,36]:

$$\nu_w = 0.02540 \times \frac{kW}{AtD} \tag{1}$$

where, k is a constant (3.45×10^6), W is the weight loss (g), A is the area of the specimen (cm^2), t is the time of exposure (h) and D is the density (g cm^{-3}). The values of inhibition efficiency (η'%) were calculated using the formula:

$$\eta'\% = \frac{W_{corr} - W_{inh}}{W_{corr}} \times 100 \tag{2}$$

Here, W_{corr} and W_{inh} (in g) are the weight losses of mild steel in an uninhibited and an inhibited systems, respectively.

2.6. Electrochemical corrosion studies

Electrochemical measurements were performed using the Electrochemical Workstation (Model No: CHI 760, CH Instruments, USA) and all the experiments were carried out at a constant temperature of 28 ± 1 °C with ground water as electrolyte. A platinum electrode along with a saturated calomel electrode (SCE) was used as auxiliary and reference electrodes, respectively and the working electrodes composed of the mild steel specimens of 1 cm^2 exposed area. The tip of the reference electrode was positioned very close to the surface of the working electrode with the use of a fine Luggin capillary in order to minimise the ohmic potential drop. The remaining uncompensated resistance was also reduced by using the electrochemical workstation.

The open circuit potential (OCP) of the mild steel specimens in the absence and presence of inhibitors was monitored as a function of time during 192 h to analyse their corrosion behaviour under free corrosion potential conditions in the ground water medium. Polarization experiments were performed by using an initial delay time at the equilibrium state of 1 h in order to stabilize mild steel surface at OCP. Potentiodynamic polarisation studies of uninhibited and inhibited mild steel specimens were carried out in the potential range of −1000 to 200 mV vs. SCE at a scan rate of 0.1 mV s^{-1}.

The electrochemical impedance studies were carried out using the same setup as that of potentiodynamic polarisation studies, and the applied AC perturbation signal was 10 mV within the frequency range between 10^5 Hz and 10^{-2} Hz. Corrosion current, potential and corrosion rates were determined with the Tafel extrapolation method. All the electrochemical impedance measurements were carried out at OCP. All the tests were performed under aerated condition. Three replicas of each experiment were carried out and the reproducibility was good.

2.7. Quantum chemical calculations

DFT has the merit of including the relativistic effects as an electron correlation term and thus it holds well among the other quantum chemical methods. The molecular structure of the newly synthesised compounds were performed using DFT [37] along with 6-311G** basis set. All these calculations were performed using Gaussian 03 software package [38]. A combination of Becke's three-parameter (B3) [39,40] exchange functional and Lee, Yang and Parr (LYP) gradient-corrected correlation functional i.e., B3LYP hybrid functional is used for the entire calculations. The isosurface representation of molecular orbitals such as HOMO, LUMO structures of the inhibitors were obtained using GVIEW program [41–45].

Trying to get insight into the molecular dynamic simulation, some of the quantum chemical parameters such as susceptibility χ, chemical potential Pi, energy gap ΔE, global hardness η, softness σ and dipole moment μ were calculated. Frequency analysis was performed to ensure the calculated structure being the minimum on the potential energy surface (without imaginary frequency). The concepts of these parameters are related to each other as follows [46–52]:

$$\mathrm{Pi} = -\chi \tag{3}$$

$$\mathrm{Pi} = \frac{E_{HOMO} + E_{LUMO}}{2} \tag{4}$$

$$\eta = \frac{E_{HOMO} - E_{LUMO}}{2} \tag{5}$$

$$\Delta E = E_{LUMO} - E_{HOMO} \tag{6}$$

$$\sigma = \frac{1}{\eta} \tag{7}$$

According to frontier molecular orbital theory (FMO), the chemical reactivity is a function of interaction between HOMO

and LUMO levels of reacting species [50]. The E_{HOMO} indicates the ability of the molecule to donate electrons to the appropriated E_{LUMO} acceptor and E_{LUMO} indicates its ability to accept electrons. The lower the value of energy gap ΔE, the more ability of the molecule is to accept electrons. While the higher is the value of ΔE of the inhibitor, the easier it offers electrons to the unoccupied d-orbital of metal surface and the greater is its inhibition efficiency.

3. Results and discussion

3.1. Gravimetric analysis

The effect of the imidazole derivatives on inhibiting the corrosion of mild steel in ground water medium was studied by measuring the weight loss of the specimens at room temperature. Fig. 2(a) and (b) show the representative plots of corrosion rate against time (h) for mild steel in ground water medium in the absence and presence of different concentrations of BIDM and TITM whereas Fig. 2(c) and (d) correspond to the plots of inhibition efficiency vs. concentration of BIDM and TITM, respectively. From the results it can be inferred that, as the concentration of the inhibitor increases the inhibition efficiency increases along with a reduction in corrosion rate for the mild steel specimens in the presence of BIDM and TITM than that in their absence. But it is noticed that there is a significant decrease in corrosion rate up to the optimum level of concentration 0.67 mM for BIDM and 0.49 mM for TITM whereas the concentrations beyond optimum shows a slight appreciation (Fig. 2(a) and (b)). The optimum concentration for BIDM provided the inhibition efficiency of 79% and 89% for TITM. These inhibition efficiencies could be due to the adsorption of both the imidazoles on to the mild steel surface through the lone pair of

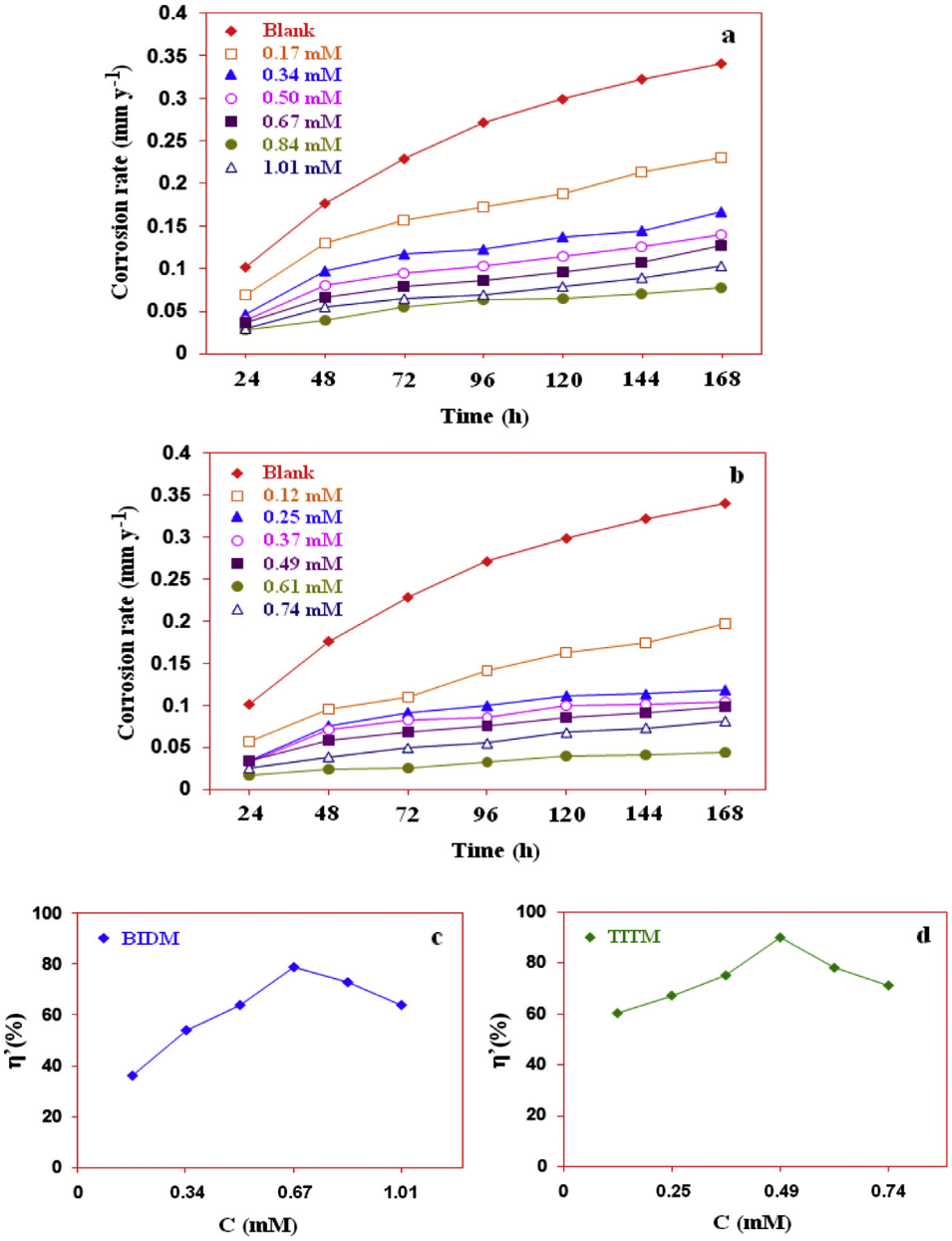

Fig. 2. Plots obtained for mild steel in ground water medium in the absence and presence of BIDM and TITM: (a) and (b) corrosion rate vs. time; (c) and (d) inhibition efficiency vs. concentration.

electrons present in nitrogen atoms which easily involves the donor acceptor interaction as could be inferred from quantum chemical studies [40]. The presence of substituent in the form of bipodal (BIDM) and tripodal (TITM) imidazoles could attribute to the increased surface area coverage by the adsorption phenomenon on the metal surface.

3.2. Electrochemical characterizations

3.2.1. OCP and polarisation measurements

The OCP-time measurements of mild steel in ground water medium in the absence and presence of inhibitors like BIDM and TITM, respectively was carried out during the immersion time period of 192 h and the corresponding OCP values are presented in Table 1. Fig. 3 shows the OCP of mild steel in the ground water medium with the optimum concentration of inhibitors during the immersion time period of 192 h, while the inset in Fig. 3 shows the OCP of mild steel during the first 1 h of immersion time. From the measurements, it was inferred that the steady state potential of −0.61 V vs. SCE for mild steel in ground water medium in the absence of inhibitor was attained after an hour of immersion. Whereas, in the presence of inhibitors at the optimum concentrations of 0.67 mM for BIDM and 0.49 mM for TITM, the steady state potential of −0.50 V vs. SCE and −0.48 V vs. SCE, respectively was attained within 10 min of immersion time which demonstrates the protective effect of BIDM and TITM in the ground water medium. Thus, the protection of mild steel from corrosion is evidenced by the improved surface coverage of inhibitor molecule on mild steel surface.

3.2.2. Potentiodynamic polarisation studies

The potentiodynamic polarisation curves of mild steel specimen in the ground water medium in the absence and presence of different concentrations of BIDM and TITM are shown in Fig. 4(a) and (b). The corrosion kinetic parameters such as corrosion potential (E_{corr}) and corrosion current density (i_{corr}) were deduced from the curves obtained from the polarisation measurements and their values are presented in Table 1. We obtain the corrosion current density (i_{corr}) by extrapolating the Tafel lines to the corrosion potential. The uninhibited mild steel specimen exhibits an E_{corr} value around −0.65 mV vs. SCE with an i_{corr} value of 36.6 μA cm^{-2}. The polarisation plots presented in Fig. 4(a) and (b) reveal that on adding the imidazole derivatives the cathodic and anodic branches are shifted towards lower current density, which could be due to the adsorbed inhibitor molecules that effectively block the available reaction sites on metal surface. No significant changes were observed for the E_{corr} values except for the 1.01 mM (BIDM) and 0.74 (TITM), also the values shift to the positive direction in the presence of the inhibitors when compared to that of the blank. This consistency in E_{corr} may seem to exhibit control on both cathodic as well as anodic reaction and thus they act as mixed type inhibitors. In particular TITM has E_{corr} values that shift more positive for 0.12 mM and move towards the negative direction for the subsequent concentrations, which evidenced the decrease in the rate of cathodic reaction. As can be seen in Table 1, the value of η'% seems to be increasing up to the optimum concentration of the inhibitors (0.67 mM for BIDM and 0.49 mM for TITM). The values of η'% were calculated using the following equation:

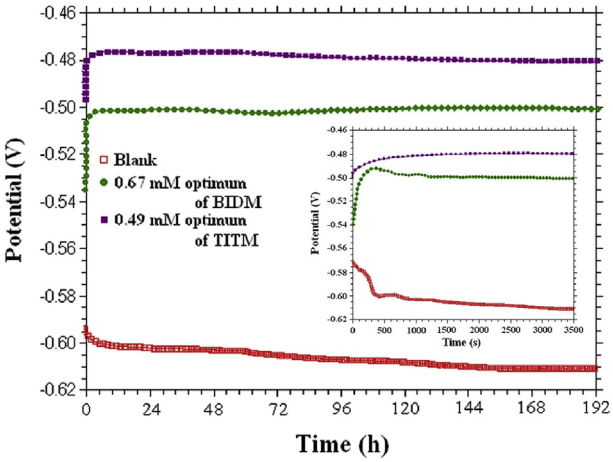

Fig. 3. OCP time plots obtained for mild steel in ground water medium in the absence and presence of BIDM and TITM. [Inset: OCP plots during 1 h immersion time].

$$\eta'\% = \frac{\nu - \nu'}{\nu} \times 100 \quad (8)$$

where, ν and ν' are the corrosion rate values for uninhibited and inhibited systems, respectively. The values of ν and ν' were estimated according to the previous report [53]. The parallel cathodic Tafel curves in Fig. 4 suggest that the hydrogen evolution is activation-controlled and the reduction mechanism is not affected by the presence of the inhibitors. The value of η'% for BIDM was circa 79% increased with TITM to record about 90% at the optimum concentration (0.67 mM for BIDM and 0.49 mM for TITM). The higher η'% value in case of TITM is because it possesses increased substituent with its tripodal structure. This substituent has more active sites that increase the adsorption probability for TITM

Table 1
Electrochemical parameters obtained for mild steel in ground water medium containing different concentrations of the imidazoles.

Name of the inhibitor	Concentration of inhibitor (mM)	OCP (V vs. SCE)	[a]E_{corr} (V vs. SCE)	[a]i_{corr} (μA cm^{-2})	ν (mm/year)	% η'
–	0	−0.61	−0.65	36.6	0.407	–
BIDM	0.17	−0.57	−0.63	23.6	0.262	36
	0.34	−0.55	−0.60	16.9	0.188	54
	0.50	−0.54	−0.61	13.9	0.154	62
	0.67	−0.50	−0.60	7.5	0.083	79
	0.84	−0.52	−0.60	9.8	0.109	73
	1.01	−0.51	−0.54	13.2	0.147	64
TITM	0.12	−0.51	−0.64	14.1	0.157	60
	0.25	−0.53	−0.62	12.4	0.138	67
	0.37	−0.55	−0.59	9.0	0.100	75
	0.49	−0.48	−0.53	4.1	0.046	90
	0.61	−0.57	−0.68	6.3	0.070	78
	0.74	−0.59	−0.69	10.0	0.111	71

[a] Based on the Tafel extrapolation method.

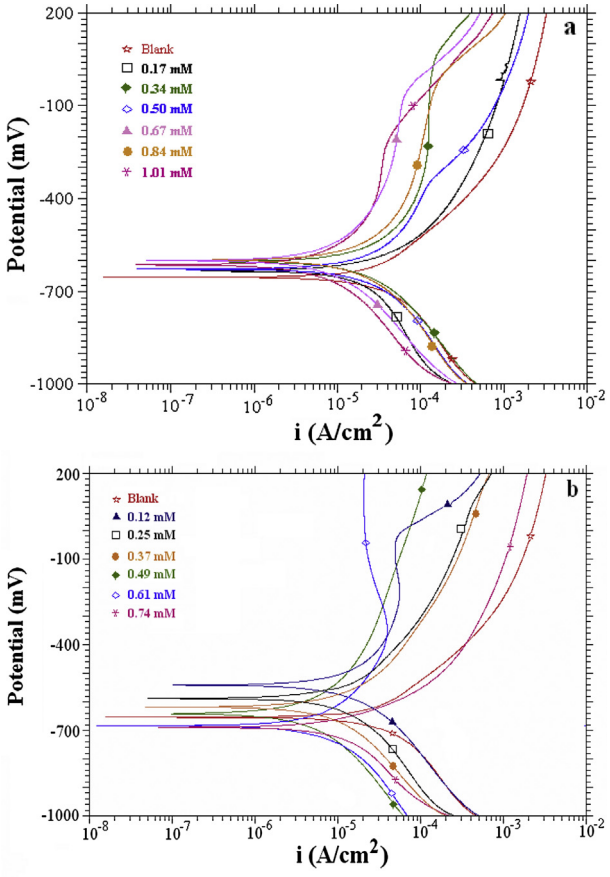

Fig. 4. Potentiodynamic polarisation curves for mild steel in ground water containing different concentrations of (a) BIDM and (b) TITM.

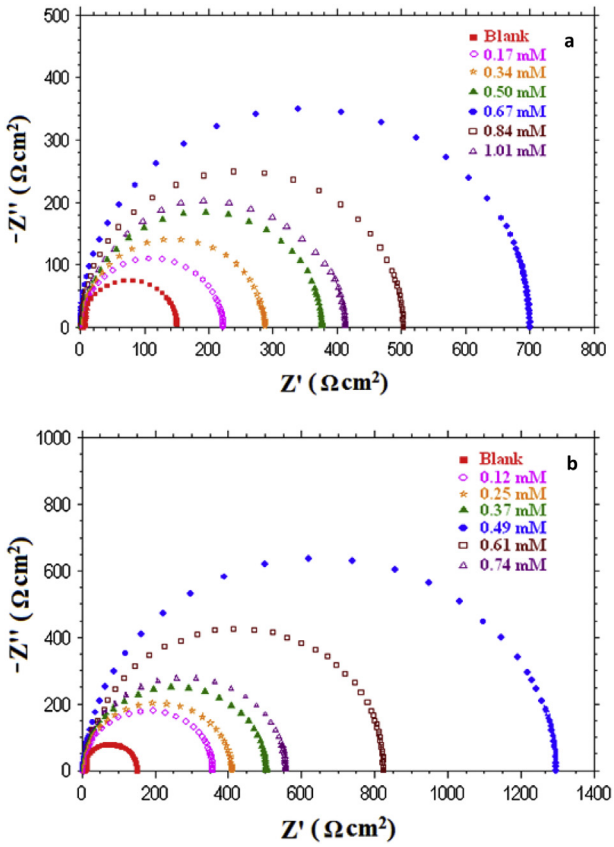

Fig. 5. Nyquist plots for mild steel in ground water containing different concentrations of (a) BIDM and (b) TITM.

molecules on the steel, which in turn blocks the weak parts and flawed areas of the surface precluding its corrosion. Thus the polarisation results emphasise that TITM with its tripodal like structure, behaves as a better corrosion inhibitor.

3.2.3. Electrochemical impedance studies

The Nyquist plots for mild steel in ground water medium containing different concentrations of the BIDM and TITM are given in Fig. 5(a) and (b). The equivalent circuit used to fit the Nyquist plot is given in Fig. 6. The first element in the circuit denotes solution resistance (R_s), which corresponds to the ohmic resistance of the system, whereas R_1 represents the charge transfer resistance and R_2 belongs to the resistance exhibited by the impervious layer of the inhibitor. The values of C_{dl_1} and C_{dl_2} correspond to the double layer capacitance and the capacitance of the inhibitor layer, respectively. The presence of inhibitors does not alter the profile of the impedance behaviour which suggests a similar mechanism for the mild steel corrosion inhibition process using both the imidazole derivatives. Moreover, the impedance spectra show single semicircle and the diameter of the semicircle increases with increasing inhibitor concentration. These plots show that the impedance spectra consist of one capacitive loop at high frequency, which was attributed to single charge transfer of the corrosion process. Then, it is noticed that the impedance spectra show a "depressed" semicircle at the centre under the real axis, such phenomenon often refer to the frequency dispersion of interfacial impedance which has been attributed to the roughness, in homogeneity of the solid surfaces and adsorption of inhibitors.

The capacitance (C_{dl}) and the charge transfer resistance (R_{ct}) were calculated from the Nyquist plots and presented in Table 2. In the case of the electrochemical impedance spectroscopy, the inhibition efficiency is calculated using the charge transfer resistance values as follows [54]:

$$\eta'\% = \frac{R_{ct}^{inh} - R_{ct}}{R_{ct}^{inh}} \times 100 \quad (9)$$

where, R_{ct} and R_{ct}^{inh} are the charge transfer resistance values for mild steel in the absence and presence of the inhibitors in the ground water medium. The diameter of the semicircle evidenced a marked increase while compared with the blank whose R_{ct} value is 133 Ω cm^2. This shows that the larger charge transfer resistance values for the optimum evidenced a slower corroding system. Decrease in the capacitance value C_{dl} for the optimum concentration (0.67 mM for BIDM and 0.49 mM for TITM) could have resulted

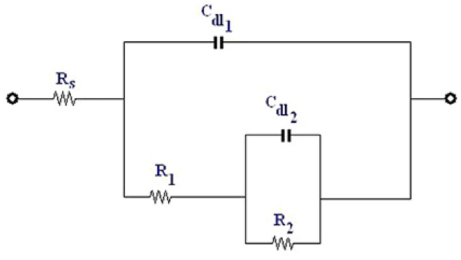

Fig. 6. Equivalent circuit model used to fit the EIS data presented in Fig. 5.

Table 2
Electrochemical impedance parameters for mild steel in ground water containing different concentrations of the imidazoles.

Name of the inhibitor	Concentration of inhibitor (mM)	C_{dl} (μF cm^{-2})	R_{ct} (Ω cm^2)	$\tau_d \times 10^{-2}$ (S)	%η
–	0	31.9	133	0.424	–
BIDM	0.17	20.3	207	0.420	36
	0.34	14.9	281	0.419	53
	0.50	12.4	340	0.422	61
	0.67	6.1	687	0.419	80
	0.84	8.7	491	0.427	73
	1.01	11.6	368	0.427	64
TITM	0.12	12.7	335	0.425	60
	0.25	10.6	406	0.430	67
	0.37	7.5	549	0.412	76
	0.49	3.1	1265	0.392	90
	0.61	5.8	811	0.470	82
	0.74	8.5	498	0.423	73

due to the local dielectric constant decrease and/or the increase in thickness of the electrical double layer which strictly suggests that these molecules of BIDM and TITM act by adsorption on the metal/solution interface [54].

The inhibitor molecules may have reduced the capacitance value on increasing the inhibitor concentration, which could be due to the increase in the double layer thickness as a consequence of replacement of water molecules by the imidazoles on the mild steel surface. This could be inferred from the Helmholtz model [55]:

$$C_{dl} = \frac{\varepsilon\varepsilon_0 A}{\delta} \tag{10}$$

where, ε is the dielectric constant of the medium and ε_0 is the vacuum permittivity, A is the electrode surface area and δ is the thickness of the protective layer. Thus the value of C_{dl} is always smaller in the presence of the inhibitor than in its absence, as a result of the effective adsorption of the imidazole derivatives. The time constant of the charge transfer process (τ_d) is defined as

$$\tau_d = C_{dl} \times R_{ct} \tag{11}$$

The inferred interface time constant value (τ) for the different concentrations of imidazoles also shows that TITM behaves as a better corrosion inhibitor than BIDM. The τ value is possibly high when the corrosion inhibitors are added to the aqueous medium and thus the value of τ can be used to evaluate the inhibitor adsorption process on the electrode surface. The observed values suggest that the amount of accumulated charge per unit on electrode surface with TITM is lower than BIDM. Thus the result obtained from EIS is corroborative with the potentiodynamic polarisation and weight loss measurements.

3.3. Quantum chemical calculations

Quantum chemical calculations were carried out in order to investigate the adsorption and inhibition mechanism that relates the molecular structure of the present inhibitor and its inhibiting effect. Fig. 7(a) and (b) shows the optimised geometry of the BIDM and TITM molecules and their horizontal *G* view at 45° steric is given in Fig. 7(c) and (d). Quantum chemical indices containing E_{HOMO}, E_{LUMO} and other parameters have been presented in Table 3 and the bond parameters such as bond distance, bond length and dihedral angles are given in Table 4. Figs. 8 and 9 show the HOMO and LUMO structures of the imidazole derivatives.

According to the frontier molecular orbital (FMO) theory the chemical reactivity is a function of interaction reactivity between HOMO and LUMO levels which are mainly the energies of the molecular orbital. The E_{HOMO} value of the chemical species (BIDM and TITM) thus evidenced facilitates adsorption, and therefore enhance the inhibition efficiencies by influencing the transport process through the adsorbed layer. The energy of the E_{LUMO} indicates the ability of the molecule to accept electrons and thus these are in the acceptor states. While comparing the FMO results of BIDM and TITM their E_{HOMO} values didn't show any marked variation, whereas their E_{LUMO} values shows that the TITM has a

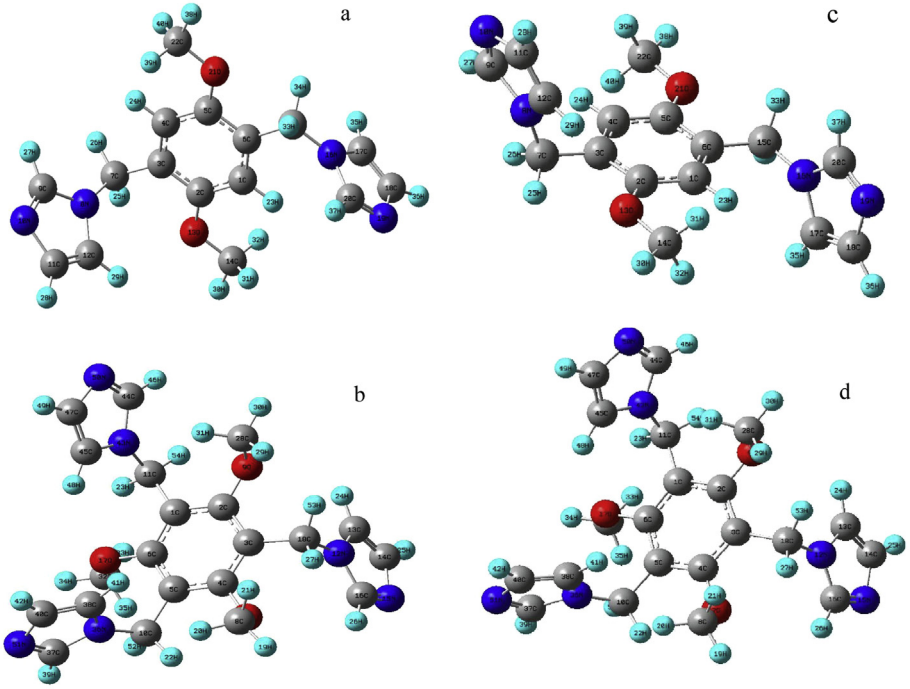

Fig. 7. Optimised structures of (a) BIDM and (b) TITM and their horizontal *G* view at 45° steric for (c) BIDM and (d) TITM.

Table 3
Selected geometrical parameters.

BIDM			TITM		
Bond length	Bond angle (°)	Dihedral angle (°)	Bond length	Bond angle (°)	Dihedral angle (°)
$C_1–C_2 = 1.398$	$C_1–C_2–C_3 = 119.9$	$C_1–C_2–C_3–C_4 = -0.7$	$C_1–C_2 = 1.403$	$C_1–C_2–C_3 = 121.7$	$C_1–C_2–C_3–C_4 = -4.7$
$C_2–C_3 = 1.401$	$C_2–C_3–C_4 = 119.0$	$C_2–C_3–C_4–C_5 = 0.1$	$C_2–C_3 = 1.400$	$C_2–C_3–C_4 = 118.2$	$C_2–C_3–C_4–C_5 = 3.6$
$C_3–C_4 = 1.396$	$C_3–C_4–C_5 = 121.2$	$C_3–C_4–C_5–C_6 = 0.6$	$C_3–C_4 = 1.402$	$C_3–C_4–C_5 = 121.7$	$C_3–C_4–C_5–C_6 = 0.8$
$C_4–C_5 = 1.393$	$C_4–C_5–C_6 = 119.8$	$C_4–C_5–C_6–C_1 = -0.7$	$C_4–C_5 = 1.401$	$C_4–C_5–C_6 = 118.0$	$C_4–C_5–C_6–C_1 = -4.3$
$C_5–C_6 = 1.403$	$C_1–C_6–C_5 = 119.2$	$C_2–C_1–C_6–C_5 = 0.1$	$C_5–C_6 = 1.403$	$C_1–C_6–C_5 = 122.0$	$C_2–C_1–C_6–C_5 = 3.3$
$C_1–C_6 = 1.391$	$C_2–C_1–C_6 = 121.0$	$C_6–C_1–C_2–C_3 = 0.6$	$C_1–C_6 = 1.399$	$C_2–C_1–C_6 = 118.1$	$C_6–C_1–C_2–C_3 = 1.4$
$C_3–C_7 = 1.514$	$C_2–C_3–C_7 = 120.7$	$C_1–C_2–C_3–C_7 = 179.7$	$C_4–O_7 = 1.381$	$C_3–C_4–O_7 = 118.6$	$O_7–C_4–C_5–C_6 = -175.5$
$C_7–N_8 = 1.464$	$C_4–C_3–C_7 = 120.3$	$C_2–C_3–C_7–N_8 = 94.4$	$O_7–C_8 = 1.435$	$C_5–C_4–O_7 = 119.6$	$C_3–C_4–O_7–C_8 = 91.0$
$N_8–C_9 = 1.368$	$C_3–C_7–N_8 = 113.6$	$C_4–C_3–C_7–C_8 = -85.1$	$C_2–O_9 = 1.379$	$C_4–O_7–C_8 = 115.7$	$C_5–C_4–O_7–C_8 = -92.5$
$C_9–N_{10} = 1.313$	$C_7–N_8–C_9 = 126.6$	$C_3–C_7–N_8–C_9 = 107.7$	$C_5–C_{10} = 1.511$	$C_1–C_2–O_9 = 118.8$	$C_2–C_3–C_4–O_7 = 180.0$
$N_{10}–C_{11} = 1.376$	$N_8–C_9–N_{10} = 112.3$	$C_7–N_8–C_9–N_{10} = -178.2$	$C_1–C_{11} = 1.514$	$C_3–C_2–O_9 = 119.4$	$O_9–C_2–C_3–C_4 = 179.3$
$C_{11}–C_{12} = 1.371$	$C_9–N_{10}–C_{11} = 105.0$	$N_8–C_9–N_{10}–C_{11} = 0.2$	$N_{12}–C_{13} = 1.382$	$C_4–C_5–C_{10} = 120.9$	$C_6–C_1–C_2–O_9 = 177.4$
$N_8–C_{12} = 1.380$	$N_{10}–C_{11}–C_{12} = 110.7$	$C_9–N_{10}–C_{11}–C_{12} = -0.1$	$C_{13}–C_{14} = 1.370$	$C_6–C_5–C_{10} = 121.1$	$C_3–C_4–C_5–C_{10} = -179.5$
$C_2–O_{13} = 1.370$	$N_8–C_{12}–C_{11} = 105.5$	$N_{10}–C_{11}–C_{12}–N_8 = -0.1$	$C_{14}–N_{15} = 1.377$	$C_2–C_1–C_{11} = 120.9$	$O_7–C_4–C_5–C_{10} = 4.2$
$O_{13}–C_{14} = 1.424$	$C_7–N_8–C_{12} = 126.9$	$C_7–N_8–C_{12}–C_{11} = 178.1$	$N_{15}–C_{16} = 1.312$	$C_6–C_1–C_{11} = 121.0$	$C_{10}–C_5–C(6)–C_1 = 175.9$
$C_6–C_{15} = 1.519$	$C_9–N_8–C_{12} = 106.4$	$C_9–N_8–C_{12}–C_{11} = 0.2$	$N_{12}–C_{16} = 1.369$	$N_{12}–C_{13}–C_{14} = 105.5$	$C_{11}–C_1–C_2–O_9 = -1.4$
$C_{15}–N_{16} = 1.454$	$C_1–C_2–O_{13} = 123.7$	$C_7–C_3–C_4–C_5 = 179.7$	$C_6–O_{17} = 1.378$	$C_{13}–C_{14}–N_{15} = 110.7$	$C_{11}–C_1–C_2–C_3 = -177.4$
$N_{16}–C_{17} = 1.381$	$C_3–C_2–O_{13} = 116.4$	$C_{12}–N_8–C_9–N_{10} = -0.3$	$C_3–C_{18} = 1.517$	$C_{14}–N_{15}–C_{16} = 105.2$	$C_{11}–C_1–C_6–C_5 = 178.0$
$C_{17}–C_{18} = 1.371$	$C_2–O_{13}–C_{14} = 118.7$	$C_3–C_7–N_8–C_{12} = -69.8$	$N_{12}–C_{18} = 1.463$	$N_{12}–C_{16}–N_{15} = 112.2$	$C_2–C_3–C_{18}–N_{12} = -87.4$
$C_{18}–N_{19} = 1.376$	$C_1–C_6–C_{15} = 122.5$	$O_{13}–C_2–C_3–C_4 = 178.9$	$O_9–C_{28} = 1.440$	$C_{13}–N_{12}–C_{16} = 106.5$	$C_4–C_3–C_{18}–N_{12} = 86.9$
$N_{19}–C_{20} = 1.313$	$C_5–C_6–C_{15} = 118.3$	$O_{13}–C_2–C_3–C_7 = -0.6$	$O_{17}–C_{32} = 1.434$	$C_1–C_6–O_{17} = 119.1$	$N_{12}–C_{13}–C_{14}–N_{15} = 0.3$
$N_{16}–C_{20} = 1.368$	$C_6–C_{15}–N_{16} = 114.5$	$C_6–C_1–C_2–O_{13} = -179.0$	$C_{10}–N_{36} = 1.466$	$C_5–C_6–O_{17} = 118.8$	$C_{13}–C_{14}–N_{15}–C_{16} = 0.1$
$C_5–O_{21} = 1.370$	$C_{15}–N_{16}–C_{17} = 126.8$	$C_1–C_2–O_{13}–C_{14} = -4.0$	$N_{36}–C_{37} = 1.366$	$C_{13}–N_{12}–C_{18} = 126.6$	$C_{14}–N_{15}–C_{16}–N_{12} = -0.4$
$O_{21}–C_{22} = 1.422$	$N_{16}–C_{17}–C_{18} = 105.7$	$C_3–C_2–O_{13}–C_{14} = 176.4$	$N_{36}–C_{38} = 1.381$	$C_{16}–N_{12}–C_{18} = 126.8$	$C_{16}–N_{12}–C_{13}–C_{14} = -0.5$
	$C_{17}–C_{18}–N_{19} = 110.6$	$C_4–C_5–C_6–C_{15} = 180.0$	$C_{38}–C_{40} = 1.372$	$C_2–C_3–C_{18} = 121.0$	$C_{13}–N_{12}–C_{16}–N_{15} = 0.6$
	$C_{18}–N_{19}–C_{20} = 105.1$	$C_2–C_1–C_6–C_{15} = 179.4$	$C_{11}–N_{43} = 1.465$	$C_4–C_3–C_{18} = 120.5$	$C_{13}–N_{12}–C_{18}–C_3 = 80.2$
	$N_{16}–C_{20}–N_{19} = 112.3$	$C_1–C_6–C_{15}–N_{16} = 6.4$	$N_{43}–C_{44} = 1.369$	$C_3–C_{18}–N_{12} = 112.4$	$C_{18}–N_{12}–C_{16}–N_{15} = 178.0$
	$C_{15}–N_{16}–C_{20} = 126.8$	$C_5–C_6–C_{15}–N_{16} = -174.4$	$N_{43}–C_{45} = 1.381$	$C_2–O_9–C_{28} = 115.3$	$C_{18}–N_{12}–C_{13}–C_{14} = -177.9$
	$C_{17}–N_{16}–C_{20} = 106.3$	$C_6–C_{15}–N_{16}–C_{17} = 81.8$	$C_{45}–C_{47} = 1.371$	$C_6–O_{17}–C_{32} = 115.8$	$C_{16}–N_{12}–C_{18}–C_3 = -96.7$
	$C_5–O_{21}–C_{22} = 118.6$	$C_{15}–N_{16}–C_{17}–C_{18} = -176.8$	$C_{47}–N_{50} = 1.376$	$C_5–C_{10}–N_{36} = 113.5$	$C_4–C_5–C_6–O_{17} = 179.7$
	$C_4–C_5–O_{21} = 124.8$	$N_{16}–C_{17}–C_{18}–N_{19} = 0.2$	$C_{44}–N_{50} = 1.313$	$C_{10}–N_{36}–C_{37} = 125.7$	$C_{10}–C_5–C_6–O_{17} = 0.0$
	$C_6–C_5–O_{21} = 115.4$	$C_{17}–C_{18}–N_{19}–C_{20} = 0.0$	$C_{40}–N_{51} = 1.374$	$C_{10}–N_{36}–C_{38} = 127.9$	$C2–C1–C_6–O_{17} = -179.2$
		$C_{18}–N_{19}–C_{20}–N_{16} = -0.2$	$C_{37}–N_{51} = 1.313$	$C_{37}–N_{36}–C_{38} = 106.3$	$C_{11}–C_1–C_6–O_{17} = -2.0$
		$C_{17}–N_{16}–C_{20}–N_{19} = 0.3$		$N_{36}–C_{38}–C_{40} = 105.6$	$C_1–C_2–C_3–C_{18} = 169.7$
		$C_{15}–N_{16}–C_{20}–N_{19} = 176.8$		$C_1–C_{11}–N_{43} = 113.6$	$O_9–C_2–C_3–C_{18} = -6.2$
		$C_6–C_{15}–N_{16}–C_{20} = -93.9$		$C_{11}–N_{43}–C_{44} = 126.3$	$C_{18}–C_3–C_4–C_5 = -170.9$
		$C_{20}–N_{16}–C_{17}–C_{18} = -0.3$		$C_{11}–N_{43}–C_{45} = 127.2$	$C_{18}–C_3–C_4–O_7 = 5.5$
		$O_{21}–C_5–C_6–C_1 = 179.5$		$C_{44}–N_{43}–C_{45} = 106.5$	$C_1–C_2–O_9–C_{28} = 97.7$
		$O_{21}–C_5–C_6–C_{15} = 0.2$		$N_{43}–C_{44}–N_{50} = 112.3$	$C_3–C_2–O_9–C_{28} = -86.2$
		$O_3–C_4–C_5–O_{21} = -179.6$		$C_{45}–C_{47}–N_{50} = 110.7$	$C_1–C_6–O_{17}–C_{32} = 93.8$
		$C_4–C_5–O_{21}–C_{22} = 1.4$		$N_{43}–C_{45}–C_{47} = 105.4$	$C_5–C_6–O_{17}–C_{32} = -90.1$
		$C_6–C_5–O_{21}–C_{22} = -178.9$		$C_{44}–N_{50}–C_{47} = 105.1$	$C_4–C_5–C_{10}–N_{36} = 114.5$
				$C_{37}–N_{51}–C_{40} = 105.1$	$C_6–C_5–C_{10}–N_{36} = -65.8$
				$C_{38}–C_{40}–N_{51} = 110.6$	$C_5–C_{10}–N_{36}–C_{37} = 144.6$
					$C_5–C_{10}–N_{36}–C_{38} = -39.4$
					$C_{10}–N_{36}–C_{38}–C_{40} = -176.8$
					$C_{37}–N_{36}–C_{38}–C_{40} = -0.1$
					$N_{36}–C_{37}–N_{51}–C_{40} = 0.0$
					$C_{38}–C_{40}–N_{51}–C_{37} = -0.1$
					$C_2–C_1–C_{11}–N_{43} = -87.1$
					$C_6–C_1–C_{11}–N_{43} = 94.2$
					$C_{45}–C_{47}–N_{50}–C_{44} = 0.1$
					$C_1–C_{11}–N_{43}–C_{44} = 126.1$
					$C_1–C_{11}–N_{43}–C_{45} = -56.0$
					$N_{43}–C_{44}–N_{50}–C_{47} = -0.4$
					$C_{44}–N_{43}–C_{45}–C_{47} = -0.5$
					$C_{11}–N_{43}–C_{45}–C_{47} = -178.8$
					$C_{45}–N_{43}–C_{44}–N_{50} = 0.6$
					$N_{43}–C_{45}–C_{47}–N_{50} = 0.2$
					$C_{11}–N_{43}–C_{44}–N_{50} = 178.9$
					$N_{36}–C_{38}–C_{40}–N_{51} = 0.1$
					$C_{38}–N_{36}–C_{37}–N_{51} = 0.1$
					$C_{10}–N_{36}–C_{37}–N_{51} = 176.9$

possible low value of −1.368 eV and TITM possess −0.911 eV that evidenced a greater adsorption ability. Thus, the excellent inhibition towards corrosion are reported to be obtained using organic compounds that not only offer electrons to unoccupied orbital of the metal, but also accept free electrons from the metal by using their anti-bond orbital to form stable chelates [55]. This dynamic behaviour is observed in these two inhibitors and hence TITM with lower E_{LUMO} value gives higher inhibition efficiency.

The adsorption of organic inhibitor on the metal surface not only correlates with the energy of HOMO and LUMO, but also largely depends on the density distribution of certain orbital where the effective adsorption may occur.

Table 4
Quantum chemical parameters for the imidazoles.

Electronic properties	BIDM		TITM	
	Gaseous phase	Aqueous phase	Gaseous phase	Aqueous phase
E_{HOMO} (eV)	−6.034	−5.984	−6.264	−6.207
E_{LUMO} (eV)	−0.911	−0.921	−1.368	−1.393
Pi (eV)	−3.4725	−3.4525	−3.816	−3.800
χ (eV)	3.4725	3.4525	3.816	3 0.800
η (eV)	−2.5615	−2.5315	−2.448	−2.407
σ (eV^{-1})	−0.3904	−0.3950	−0.4085	−0.4155
ΔE (eV)	5.123	5.063	4.896	4.814
μ (debye)	4.6156	4.6283	1.728	2.165

Absolute hardness and softness are important properties to measure the molecular stability and reactivity. A hard molecule has the large energy gap and a soft molecule has a small energy. Soft molecules are more reactive than harder ones because they could easily offer electrons to the acceptor [44]. Moreover the rate of corrosion could be similarly related to the equation, $\Delta E = E_{HOMO} - E_{LUMO}$ [56–60]. The energy gap $\Delta E = 5.123$ eV for BIDM whose value is greater than that of TITM ($\Delta E = 4.896$ eV) and hence the lower value of ΔE for TITM supports the easy electron transfer between its molecular orbital which could be attributed to its better inhibition efficiency. It is also observed that TITM has a low global hardness value $\eta = -2.448$ eV than BIDM and thus, TITM by being a soft molecule would enhance adsorption on the mild steel.

The optimised molecular structures of BIDM and TITM and the high occupied molecular orbital (HOMO) demonstrate that the nitrogen atoms have a larger electron density with its lone pair of electrons which would preferably donate electrons to partially filled or vacant d orbitals of the metal resulting in donor-acceptor bond [25,60]. Molecules of BIDM can be directly adsorbed at the steel surface on the basis of donor-acceptor interactions between the non bonding lone pairs of N atoms in the bipodal like structure and vacant d-orbital of iron atoms. In fact, the tripodal like structure prevails an increased corrosion inhibition due to the at most surface coverage on the mild steel.

On calculating the values of I and A obtained from quantum chemical calculations, as well as implying the theoretical χ value of 7 eV mol^{-1} according to Pearson electronegativity scale [47] and a global hardness value of 0 eV mol^{-1} for Fe by assuming as $I = A$ for a metallic bulk, ΔN, the fraction of electrons transferred from inhibitor to the mild steel surface is obtained.

$$\Delta N = \frac{\chi_{Fe} - \chi_{inh}}{2(\eta_{Fe} + \eta_{inh})} \tag{12}$$

Both the inhibitors have $\Delta N < 3.6$ and thus the inhibition efficiency seemed to have increased with the increased electron donating ability at the metal surface [61–63]. Also the electronegativity is higher for TITM (3.816 eV) which evidence the more electron transfer than that of BIDM. These quantities are related to the ionization potential I and electron affinity A as follows:

$$\chi = \frac{I + A}{2} \tag{13}$$

$$\eta = \frac{I - A}{2} \tag{14}$$

where, $I = -E_{HOMO}$ and $A = -E_{LUMO}$. Thus constructing a composite index of an inhibitor molecule, it may be important to focus on parameters that directly influence the electronic interaction of the inhibitor molecules with the metal surface and help to predict chemical behaviour of the imidazoles.

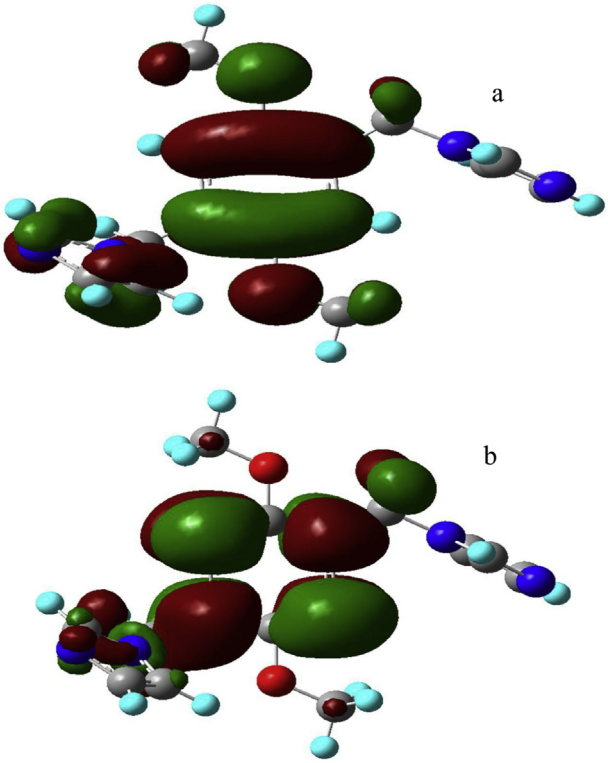

Fig. 8. (a) HOMO and (b) LUMO structures of BIDM.

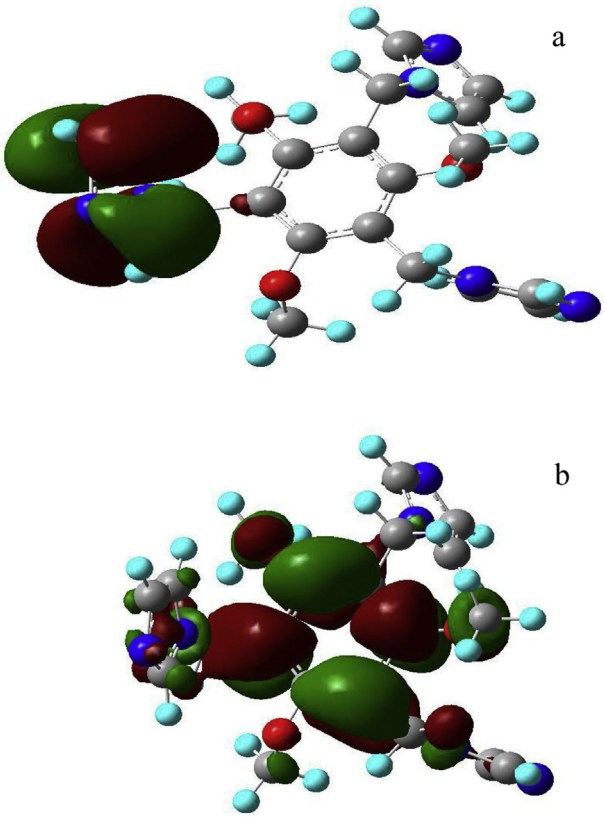

Fig. 9. (a) HOMO and (b) LUMO structures of TITM.

The solvent effect and the molecular structure could be studied by a model, which is known as Polarised Continuum Model (PCM) using Gaussian 03 program. The calculated quantum chemical parameters in the presence of a solvent (water) do not exhibit important differences. However, a slight increase in the values of E_{HOMO}, Pi, η, μ and a slight decrease in E_{LUMO}, χ, σ, ΔE are noticed in Table 4.

While studying the electrochemical behaviour of BIDM and TITM, the concentration level of BIDM was varied from 0.17 mM to 1.01 mM whereas, for TITM, the concentration level ranged between 0.12 mM and 0.74 mM. As evidenced from Table 1 and Fig. 4 the values of η'% were increasing up to the concentration of 0.67 mM after which the values of η'% decreased, indicating that 0.67 mM is the optimum concentration of BIDM. In the same way, TITM is found to have its optimum concentration of 0.49 mM. Therefore, the optimum concentrations of inhibitors were evaluated based on their inhibition efficiencies. The enhanced inhibition efficiency could be assigned to the interaction between the unshared electron pairs of heteroatom like N and the vacant d-orbital of the surface iron atoms which aids a strong adsorption to the metal surface with its bipodal and tripodal structure.

The optimized structures of these inhibitors are shown in Fig. 7(a) and (b) and the corresponding quantum chemical parameters are also listed in Table 4. As evidenced from Fig. 7(a) and (b), it is worth noting that in TITM, the nitrogen atoms of the two aza cycles are actively participating in the inhibition phenomenon. Whereas, the nitrogen atom in the third aza cycle partially involved in the inhibition phenomenon by being a barrier against the reach of corrosive ions towards the mild steel specimens. Hence, this may be the reason for the marginal variation in the inhibition efficiency of TITM when compared with that of BIDM.

4. Conclusions

Assessing the results of gravimetric and electrochemical techniques along with quantum chemical calculation, the following conclusions could be drawn as follows:

1. Among the newly synthesised bipodal and tripodal structured imidazole derivatives TITM (tripodal) provided an increased corrosion inhibition efficiency of 90% at its optimum concentration of 0.49 mM which could be revealed by the experimental techniques like weight loss, polarisation and impedance for mild steel corrosion in ground water medium.
2. The evaluation of polarisation measurements using these compounds BIDM and TITM exhibited its control on both cathodic and anodic reactions by adsorption on the mild steel surface.
3. Quantum chemical data obtained from 6 to 311**G basis set such as HOMO, LUMO, Pi, χ and ΔE for BIDM as well as TITM show that they adequately inhibits mild steel corrosion in the ground water medium.
4. The as-predicted structure and molecular suitability of BIDM and TITM confirm that the inhibition is due to adsorption.
5. Finally, this study shows a good correlation between the theoretical and experimental data which confirms the reliability of quantum chemical methods to investigate the inhibition of corrosion of metal surfaces.

Acknowledgements

One of the authors D. Gopi gratefully acknowledges the University Grants Commission (UGC-F No.40-64/2011 (SR)) and Defence Research and Development Organisation (DRDO, No. ERIP/ER/1103949/M/01/1513), New Delhi, India, for the financial support in the form of major research projects. L. Kavitha acknowledges the financial support from International Centre for Theoretical Physics (ICTP), Italy in the form of Junior Associateship. Also, D. Gopi and L. Kavitha acknowledge the UGC (Ref. No. F. 30-1/2013(SA-II)/RA-2012-14-NEW-SC-TAM-3240 and Ref. No. F. 30-1/2013(SA-II)/RA-2012-14-NEW-SC-TAM-3228) for the Research Awards.

References

[1] M.A. Amin, M.M. Ibrahim, Corros. Sci. 53 (2011) 873–885.
[2] M.H. Hussin, M.J. Kassim, N.N. Razali, N.H. Dahon, D. Nasshorudin, Arabian J. Chem. (2011), http://dx.doi.org/10.1016/j.arabjc.2011.07.002.
[3] Y. Tang, X. Yang, W. Yang, Y. Chen, R. Wan, Corros. Sci. 52 (2010) 242–249.
[4] S. Ramesh, S. Rajeswari, Electrochim. Acta 49 (2004) 811–820.
[5] E. Ebenso, M.M. Kabanda, L.C. Murulana, A.K. Singh, K. Shukla, Ind. Eng. Chem. Res. 51 (2012) 12940–12958. ACS Publications.
[6] E.J. Ekott, E.J. Akpabio, U.I. Etukudo, Environ. Res. J. 6 (2012) 304–307.
[7] V.S. Sastri, John Wiley and Sons, Chichester, UK, 1998, pp. 599–603.
[8] H. Keles, M. Keles, I. Dehri, O. Serindag, Mater. Chem. Phys. 112 (2008) 173–179.
[9] H.M. Abd El-Lateef, V.M. Abbasov, L.I. Aliyeva, E.E. Qasimov, I.T. Ismayilov, Mater. Chem. Phys. 142 (2013) 502–512.
[10] A. Kosari, M.H. Moayed, A. Davoodi, R. Parvizi, M. Momeni, H. Eshghi, H. Moradi, Corros. Sci. 78 (2014) 138–150.
[11] A. Espinoza-Vázquez, G.E. Negrón-Silva, R. González-Olvera, D. Angeles-Beltrán, H. Herrera-Hernández, M. Romero-Romob, M. Palomar-Pardavé, Mater. Chem. Phys., http://dx.doi.org/10.1016/j.matchemphys.2014.02.029.
[12] S.L. Granese, B.M. Rosales, C. Oviedo, J.O. Zerbino, Corros. Sci. 33 (1992) 1439–1453.
[13] A.Y. Musa, A.A.H. Kadhum, A.B. Mohamad, M.S. Takriff, Corros. Sci. 52 (2010) 3331–3340.
[14] P. Zhao, C. Zhong, L. Hunag, L. Niu, F. Zhang, Corros. Sci. 50 (2008) 2166–2171.
[15] A.Y. Musa, R.T.T. Jalgham, A.B. Mohamad, Corros. Sci. 56 (2012) 176–183.
[16] K.M. Govindaraju, D. Gopi, L. Kavitha, J. Appl. Electrochem. 39 (2009) 2345–2352.
[17] L. Fragoza-Mar, O. Olivares-Xometl, M.A. Dominique-Aguilar, E.A. Flores, P. Arellanes-Lozada, F. Jimenez-Cruz, Corros. Sci. 61 (2012) 171–184.
[18] D. Gopi, K.M. Govindaraju, S. Manimozhi, S. Ramesh, S. Rajeswari, J. Appl. Electrochem. 37 (2007) 681–689.
[19] D. Gopi, K.M. Govindaraju, V. Collins Arun Prakash, V. Manivannan, L. Kavitha, J. Appl. Electrochem. 39 (2009) 269–276.
[20] E.S. Ferreira, C. Giacomelli, F.C. Giacomelli, A. Spinelli, Mater. Chem. Phys. 83 (2004) 129–134.
[21] D. Gopi, K.M. Govindaraju, V. Collins Arun Prakash, D.M. Angeline Sakila, L. Kavitha, Corros. Sci. 51 (2009) 2259–2265.
[22] El Sayed H. El Ashry, A. El Nemr, S.A. Esawy, S. Ragab, Electrochim. Acta 51 (2006) 3957–3968.
[23] K.F. Khaled, Electrochim. Acta 53 (2008) 3484–3492.
[24] S. Xia, M. Qiu, L. Yu, F. Liu, H. Zhao, Corros. Sci. 50 (2008) 2021–2029.
[25] M.A. Quraishi, R. Sardar, Mater. Chem. Phys. 78 (2002) 425–431.
[26] A.O. Yuce, G. Kardas, Corros. Sci. 58 (2012) 86–94.
[27] D. Ozkir, K. Kayakirilmaz, E. Bayol, A.A. Gurten, F. Kandermirli, Corros. Sci. 56 (2012) 143–152.
[28] Sudheer, M.A. Quraishi, Corros. Sci. 70 (2013) 161–169.
[29] X. Zheng, S. Zhang, W. Li, L. Yin, J. He, J. Wua, Corros. Sci. 80 (2014) 383–392.
[30] K. Nebioglu, A. Melaiye, K.M. Hindi, S. Durmus, M.J. Panzner, L.A. Hogue, R.J. Mallett, C.E. Hovis, M. Coughenour, S.D. Crosby, A. Milsted, D.L. Ely, C.A. Tessier, C.L. Cannon, W.J. Youngs, J. Med. Chem. 49 (2006) 6811–6818.
[31] D. Gopi, El-Sayed M. Sherif, V. Manivannan, M. Surendiran, D. Rajeswari, L. Kavitha, Ind. Eng. Chem. Res. 53 (2014) 4286–4294.
[32] I.B. Obot, N.O. Obi-Egbedi, N.W. Odozi, Corros. Sci. 52 (2010) 923–926.
[33] I.B. Obot, N.O. Obi-Egbedi, Corros. Sci. 52 (2010) 282–285.
[34] ASTM Designation G1-03 "Standard Practice for Preparing, Cleaning, and Evaluating Corrosion Test Specimens", 2011.
[35] R. Narayan, Oxford & IBH Publishing Co., 1983, p. 4.
[36] R. Baboian, third ed., NACE International, Houston, 2002, p. 47.
[37] J.M. Seminario, P. Politzer (Eds.), Elesvier, Amsterdam, 1995.
[38] M.J. Frisch, G.W. Trucks, H.B. Schlegel, G.E. Scuseria, M.A. Robb, J.R. Cheeseman, J.A. Montgomery Jr., T. Vreven, K.N. Kudin, J.C. Burant, J.M. Millam, S.S. Iyengar, J. Tomasi, V. Barone, B. Mennucci, M. Cossi, G. Scalmani, N. Rega, G.A. Petersson, H. Nakatsuji, M. Hada, M. Ehara, K. Toyota, R. Fukuda, J. Hasegawa, M. Ishida, T. Nakajima, Y. Honda, O. Kitao, H. Nakai, M. Klene, X. Li, J.E. Knox, H.P. Hratchian, J.B. Cross, C. Adamo, J. Jaramillo, R. Gomperts, R.E. Stratmann, O. Yazyev, A.J. Austin, R. Cammi, C. Pomelli, J.W. Ochterski, P.Y. Ayala, K. Morokuma, G.A. Voth, P. Salvador, J.J. Dannenberg, V.G. Zakrzewski, S. Dapprich, A.D. Daniels, M.C. Strain, O. Farkas, D.K. Malick, A.D. Rabuck, K. Raghavachari, J.B. Foresman, J.V. Ortiz, Q. Cui, A.G. Baboul, S. Clifford, J. Cioslowski, B.B. Stefanov, G. Liu, A. Liashenko, P. Piskorz, I. Komaromi, R.L. Martin, D.J. Fox, T. Keith, M.A. Al-Laham, C.Y. Peng, A. Nanayakkara, M. Challacombe, P.M.W. Gill, B. Johnson, W. Chen, M.W. Wong, C. Gonzal-ez, J.A. Pople, Gaussian-2003, Rev. B.4, Gaussian, Inc., Pittsburgh, PA, 2003.
[39] C. Lee, W. Yang, R.G. Parr, Phys. Rev. B 37 (1988) 785–789.

[40] U. Salzner, J.B. Lagowski, P.G. Pickup, R.A. Poitier, J. Comput. Chem. 18 (1997) 1943–1953.
[41] A. Ghanbari, M.M. Attar, M. Mahdavian, Mater. Chem. Phys. 124 (2010) 1205–1209.
[42] A. Kosari, M. Momeni, R. Parvizi, M. Zakeri, M.H. Moayed, A. Davoodi, H. Eshghi, Corros. Sci. 53 (2011) 3058–3067.
[43] N.O. Obi-Egbedi, I.B. Obot, Corros. Sci. 53 (2011) 263–275.
[44] M.S. Masoud, M.K. Awad, M.A. Shaker, M.M.T. El-Tahawy, Corros. Sci. 52 (2010) 2387–2396.
[45] N.O. Eddy, S.A. Odoemelam, 39 (2009) 849–857.
[46] R.G. Parr, R.G. Pearson, J. Am. Chem. Soc. 105 (1983) 7512–7516.
[47] R.G. Pearson, Inorg. Chem. 27 (1998) 734–740.
[48] P. Geerlings, F. Dc Proft, W. Langacker, Chem. Rev. 103 (2003) 1793–1874.
[49] V.S. Sastri, J.R. Perumareddi, Corrosion 53 (1997) 617–622.
[50] G. Gece, S. Bilgic, Corros. Sci. 52 (2010) 3435–3443.
[51] A. Bellaouchou, B. Kabkab, A. Guenbour, A.B. Bachir, Prog. Org. Coat. 41 (2001) 121–127.
[52] R.G. Parr, R.A. Donelly, M. Levy, W.E. Palke, J. Chem. Phys. 68 (1978) 3801–3807.
[53] R.S. Chaudhary, A. Singh, Bull. Electrochem. 12 (1996) 585–590.
[54] E. McCafferty, N. Hackerman, J. Electrochem. Soc. 119 (1972) 146–154.
[55] E.E. Oguzie, Y. Li, F.H. Wang, Electrochim. Acta 53 (2007) 909–914.
[56] H.H. Hassan, Electrochim. Acta 51 (2006) 5966–5972.
[57] L. Herrag, B. Hammouti, S. Elkadiri, A. Aouniti, C. Jama, H. Vezin, F. Bentiss, Corros. Sci. 52 (2010) 3042–3051.
[58] K.F. Khaled, M.M. Al-Qahtani, Mater. Chem. Phys. 113 (2009) 150–158.
[59] R.M. Saleh, A.M.S. El Din, Corros. Sci. 12 (1972) 689–697.
[60] K. Fukui, T. Yonezawa, H.A. Shingu, J. Chem. Phys. 20 (1952) 722–725.
[61] N.O. Eddy, S.R. Stoyanov, E.E. Ebenso, Int. J. Electrochem. Sci. 5 (2010) 1127–1150.
[62] C.A. Mann, Trans. Electrochem. Soc. 69 (1936) 105–113.
[63] N. Hackerman, E.S. Snavely Jr., J.S. Payne Jr., J. Electrochem. Soc. 113 (1966) 677–681.